Desalination 272 (2011) 46–50

Contents lists available at ScienceDirect

Desalination

journal homepage: www.elsevier.com/locate/desal

# Synthesis and characterization of a carbon nanotube/polymer nanocomposite membrane for water treatment

Hosam A. Shawky [a,b,*], So-Ryong Chae [c], Shihong Lin [a], Mark R. Wiesner [a]

[a] Departement of Civil and Environmental Engineering, Duke University, Durham, NC 27708-0287, USA
[b] Water Treatment & Desalination Unit, Desert Research Center, El-Matariya, Cairo, P.O.B 11753, Egypt
[c] School of Chemical and Biomolecular Engineering, University of Sydney, NSW 2006, Australia

ARTICLE INFO

*Article history:*
Received 11 August 2010
Received in revised form 23 December 2010
Accepted 23 December 2010
Available online 26 January 2011

*Keywords:*
Multi-wall carbon nanotubes
Aromatic polyamide
Nanocomposite membrane
Reinforcement
Water treatment

ABSTRACT

Multi-wall carbon nanotube (MWCNT)/aromatic polyamide (PA) nanocomposite membranes were synthesized by a polymer grafting process. Surface morphology, roughness, and mechanical strength of the resultant nanocomposite membranes were characterized by scanning electron microscopy (SEM), atomic force microscopy (AFM), and micro-strain analysis, respectively. SEM and AFM images showed that MWCNTs were well dispersed in the PA matrix. Measurements of mechanical properties of this composite showed increasing membrane strength with increasing MWCNT content with monotonic increases in Young's modulus, toughness, and tensile strength. The addition of MWCNTs also improved the rejection of both salt and organic matter relative to the 10% PA membrane base case. The nanocomposite membrane synthesized with 15 mg/g MWCNT in a 10% PA casting solution rejected NaCl and humic acid by factors of 3.17 and 1.67 respectively relative to the PA membrane without MWCNTs, while membrane permeability decreased by 6.5%.



## 1. Introduction

The structure, high aspect ratio, and chemical bonding properties of carbon nanotubes combine to produce a material with electro-mechanical properties that can be exploited in polymer composites to improve the performance of flame-retarding sheets, create electrically conductive films, thin film capacitors, and a variety of light-weight, high-strength structural materials [1–3]. The wide range of possible applications for carbon nanotubes (CNTs) has been a driving force for the commercialization and industrial-scale production of high-quality single-walled (SW), double-walled (DW) and multi-walled (MW) CNTs, and as a result these materials are now readily available for incorporation into intermediate and final products as CNT/polymer composites. However, there are significant challenges in the preparation of CNT/polymer composites, particularly concerning the need to ensure adequate interfacial adhesion between the CNTs and polymers as required to ensure a uniform distribution of CNTs throughout the composite and avoid agglomerate formation [4]. Furthermore, unless the interface is carefully engineered, poor load transfer between nanotubes (in bundles) and between nanotubes and surrounding polymer chains may result in interfacial slippage [5] and compromise the mechanical strength of the composite. Approaches to addressing these challenges include chemical modification and functionalization of the CNTs [6], surfactant treatment [7], and polymer wrapping [8].

The current study considers the fabrication of porous membranes for water treatment from CNT/polymer composites where, in addition to the challenges previously noted, formulation of the composite must also address issues such as the impact on membrane porosity and the relative affinity of solvent and solutes for the membrane. We consider improvements that CNTs might bring to membranes made from aromatic polyamides (PAs), which are in themselves excellent candidates for water treatment membranes [9,10] due to their excellent dielectric properties, superior thermal stability, high strength, and flexibility. The cross-linked structure of such PAs, yields a network with relatively low chain mobility, which in turn leads to a critical void size and preferential sorption of water on the membrane surface in contact with salt water. The addition of CNTs to polymeric membranes for water treatment has been suggested as a possible strategy to reduce membrane breakage and fouling [5]. In this study, we synthesize multi-wall carbon nanotube (MWCNTs)/aromatic polyamide (PA) nanocomposite membranes by polymer grafting. N,N-dimethylacetamide (DMAc) was used as a common solvent for CNTs and the PA polymer. Benzoyl peroxide (BPO) was used as the initiator leading to the formation of free-radicals on both CNTs and PA, which produced in turn polymer-grafted nanotubes with the desired distribution in the membrane matrix. SEM and AFM imagery

* Corresponding author. Water Treatment & Desalination Unit, Desert Research Center, El-Matariya, Cairo, P.O.B 11753, Egypt. Tel.: +20 102930710; fax: +20 226389069.
*E-mail address:* shawkydrc@hotmail.com (H.A. Shawky).

0011-9164/$ – see front matter © 2011 Elsevier B.V. All rights reserved.
doi:10.1016/j.desal.2010.12.051

confirmed the homogenous distribution of the CNTs throughout the membrane matrix and FTIR confirmed the desired functionalization. The resulted membranes were characterized with respect to mechanical properties permeability of ultrapure water and rejection of salts and humic acid.

## 2. Experimental

### 2.1. Materials

N,N-dimethylacetamide (DMAc) (HPLC grade) and benzoyl peroxide were supplied from VWR and used without further purification. LiCl, *m*-phenylenediamine (99+%) and isophthaloyl chloride (99+%), analytical reagent grade (Fisher), were used as received. Multi-wall carbon nanotubes were supplied from NanoTechLabs Inc., USA, and characterized by the company as follows; purity of 95 wt.% an average diameter of 15 nm and lengths ranging from 0.5 μm to 1 μm with most of the materials closer to 1 μm.

### 2.2. Synthesis of aromatic polyamide (PA) polymer

Polymerization was carried out in a 500 mL flask with a very high-speed magnetic stirrer. A solution of 4.326 gm (0.04 mol) of *m*-phenylenediamine and 8.48 gm (0.08 mol) of sodium carbonate in 120 mL deionized water was placed in the flask. Vigorous stirring was begun and a solution of 8.12 gm (0.04 mol) of isophthaloyl chloride in 150 mL of tetrahydrofuran was rapidly poured into the flask from a beaker. Stirring was continued for 5 min. The product thus obtained is a white fibrous precipitate. The polymer was separated by filtration; washed with excess deionized water and thus dried under vacuum at 80–90 °C. The yield of polymer is about 100% of the theoretical value.

### 2.3. Synthesis of MWCNT-PA composite membrane

A polymer grafting process was used for the synthesis of MWCNT-PA composite membrane. Previous investigators have made polymer–nanotube composites by mixing the nanotubes and polymer in a suitable solvent before evaporating the solvent to form a composite film [11–17]. One of the benefits of this method is that agitation of the nanotubes added as a powder to the solvent facilitates nanotube de-aggregation and dispersion. Almost all solution-processing methods are variations on a general theme that can be summarized as: i) dispersion of nanotubes in either a solvent or polymer solution by energetic agitation; ii) mixing of nanotubes and polymer in solution by energetic agitation; iii) controlled evaporation of solvent, leaving a composite film. In general, agitation is provided by magnetic stirring, shear mixing, reflux, or, most commonly, ultrasonication.

MWCNTs were used in this study due to the relatively low cost of these materials, the ease of derivatizing the outer wall without compromising on CNT strength, and the reduced reactivity compared with single-wall (SW) CNTs [18]. For the preparation of MWCNT-PA composite membrane, MWCNTs were dispersed in DMAc solvent via ultrasonication for 2 h. DMAc solvent was prepared with lithium chloride salts (1% (wt./v)) as a casting solution for the PA membranes [9,10,19]. This DMAc LiCl solution was prepared by adding 0.1 g of LiCl to 10 mL of DMAC and heating to complete dissolution.

Aggregation of CNTs may occur during the solvent evaporation at the membrane formation step [5]. The addition of benzoyl peroxide (BPO) initiator was done with the goal of forming of free-radicals on both CNTs and PA resulting in polymer-grafted nanotubes that would be better dispersed throughout the casting solution and forming more homogenous MWCNTs-PA composite membranes. After the addition of benzoyl peroxide (BPO) initiator (0.25% (wt./v)), the mixture was heated with stirring for 3 h at 80 °C. Stirring was continued for 24 h, then the casting solution was evacuated to remove the dissolved gas, casted onto a dried clean glass Petri dish and spread with the aid of a glass rod to form a uniform thin film. A membrane thickness of 200 μm was obtained by controlling the amount of casting solution. Thus, the film was immediately placed in an oven at 90 °C for 30 min. When the solvent was completely evaporated, the Petri dish with the membrane was cooled and immersed in a deionized water bath for at least 15 h at room temperature. Four different membranes were synthesized containing 2.5, 5, 10 and 15 mg MWCNTs/g PA, respectively with a constant PA concentration of 10% by weight in the casting solution. The properties of the synthesized composite membranes were compared with those of membrane controls cast from solutions containing PA concentrations from 10% to 20% without CNTs and BPO. All membranes were stored at ambient temperature in deionized water until testing and all experiments were performed under an atmosphere of $N_2$.

### 2.4. Characterization of the MWCNT nanocomposite membranes

Characterization of functional groups on the synthesized membranes was done by Fourier transform infrared (FTIR) spectroscopy (Nicolet 8700, ThermoScientific, USA) with an Attenuated Total Reflection (ATR) unit (ZnSe crystal, 45°). Membrane samples were rinsed with deionized water and then dried in a vacuum oven before analysis. IR spectra of the membranes were recorded in transmittance mode over a wave number range of 4000 to 650 $cm^{-1}$ at 25 °C.

The hydrophilicity of the membranes was quantified by contact angle measured using the sessile drop Young–Laplace method (Kruss EasyDrop Goniometer, Hamburg, Germany) by placing a drop of DI water (NANOpure®, Barnstead, Dubuque, IA, USA) on the membrane surface. All measurements were done in triplicate and angles were measured upon immediate release of the drops to avoid error due to evaporation.

The surface morphology of the membrane was investigated by scanning probe microscope (SPM) (Digital Instruments Dimension 3100, Veeco, Woodbury, NY, USA) and scanning electron microscopy (SEM) (Superscan SSX-550, Shimadzu Co., Kyoto, Japan). The membrane surface was scanned in tapping mode with a silicon nitride probe (ORC8, Veeco Metrology) in deionized (DI) water and surface roughness parameters were calculated from the images (Nanoscope v. 6.14).

Mechanical properties of the membranes were measured using a Micro-Strain Analyzer (TA instruments RSA III, USA) with maximum force applied = 500 gm. Cross-sectional areas of samples of known width and thickness were calculated. The films were then placed between the grips of the testing machine. The grip length was 5 cm and the speed of deformation was set at the rate of 2 mm/min.

### 2.5. Membrane permeability

Water permeability tests were conducted by observing passage of ultrapure water through using flat membrane coupons at room temperature. Measurements of the volume of permeate were taken at intervals of 5 min for 1 h over a range of applied pressures of 2.9, 3.9 and 4.9 MPa in Sterlitech™ HP4750 high-pressure stirred cells with a dead-end (Sterlitech, USA) under stirred conditions. Permeability was characterized as specific flux in units of L/h $m^2$ bar.

### 2.6. Membrane rejection

The ability of the membrane to reject salt and a naturally occurring polyelectrolyte, humic acid was also evaluated in high-pressure stirred cells. Salt rejection and the accompanying permeate flux were evaluated using a feed solution of 4000 ppm aqueous NaCl solution at room temperature. Measurements of permeate volume were taken at intervals of 15 min for 1 h and at a single constant operating pressure (3.9 MPa) under stirred conditions. The concentrations of electrolyte (NaCl) in the feed and permeate over time were measured

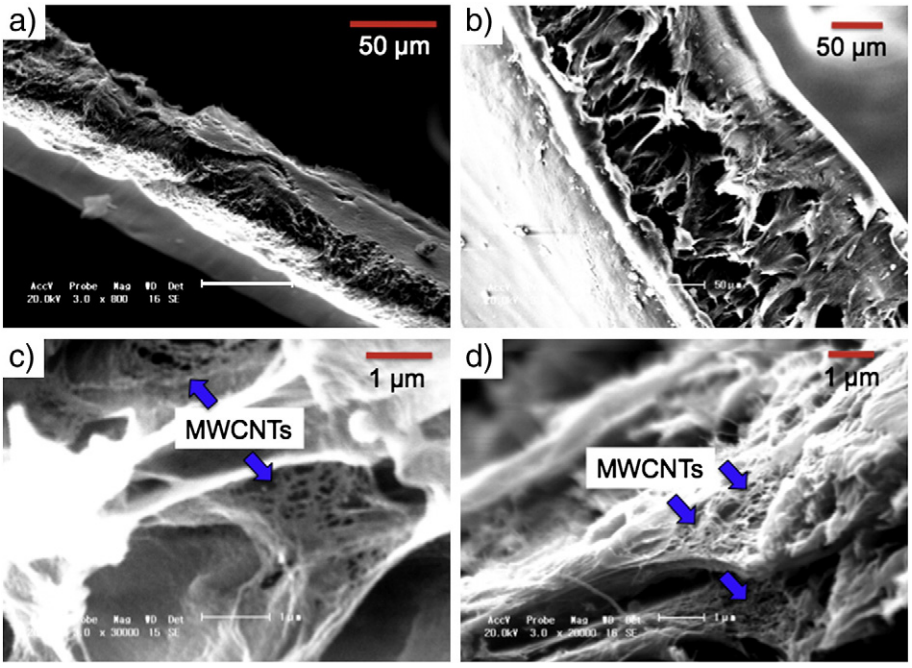


**Fig. 1.** Representative cross-sectional SEM images of a) a control membrane without MWCNTs, b) a nanocomposite membrane with 2.5 CNTs (mg/g), c) a nanocomposite membrane with 5 CNTs (mg/g), and d) a nanocomposite membrane with 15 CNTs (mg/g).

using a standardized digital conductivity meter, pH/conductivity meter model XL 20, Fisher Scientific, USA. A total of 20 mg of humic acid (Aldrich, MI, USA) was added to 1000 mL of DI water. The mixture was then filtered through the membranes at 40 bar in Sterlitech™ HP4750 high-pressure. Humic substances (UV absorbance at 254 nm) of the influent and permeate were measured by an UV/Vis spectrophotometer (U-2000, Hitachi) with a 1 cm cell.

## 3. Results and discussion

### 3.1. Synthesis of MWCNT/PA composite membrane

SEM imagery of the functionalized MWCNT in the resulting film showed MWCNTs to be well mixed and evenly distributed throughout the polymer matrix even at the highest concentration (Fig. 1) in contrast with earlier efforts to create CNT/polymer composite membranes where CNTs were non-uniformly distributed [5,20]. No evidence was observed of CNT clustering, even as CNT concentration increased to 15 mg MWCNT/g PA.

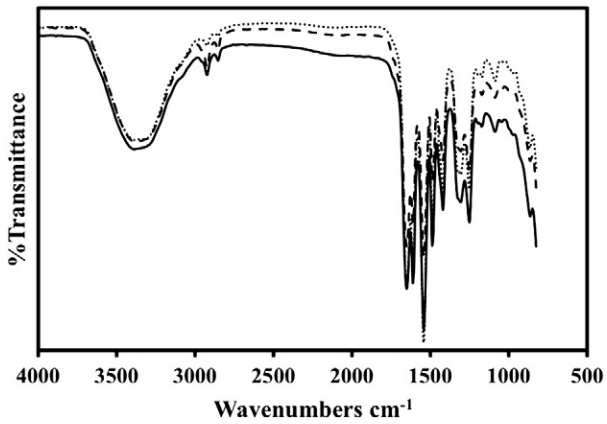


**Fig. 2.** FTIR spectra of laboratory synthesized membranes; blank PA (……), 5 mg/g MWCNTs-PA(————) and 15 mg/g (▬▬▬)MWCNTs-PA.

### 3.2. Characterization of the MWCNTs-PA nanocomposite membranes

#### 3.2.1. ATR-FTIR spectroscopy

The FT-IR spectrum of the blank membrane (Fig. 2) is quite similar to the previously published IR spectra of similar PA-membranes and shows the absence of the acid chloride band at 1770 $cm^{-1}$, indicating that successful polymerization has occurred [9,10,19]. The band at 1652.7 $cm^{-1}$ (amide I) is characteristic of the C=O stretching vibrations of the amide group. In addition, other bands characteristic of PA occur at 1541.7 $cm^{-1}$ (amide II, in-plane N–H bending and C–N stretching vibrations), 1609.6 and 1488.9 $cm^{-1}$ (aromatic ring breathing), and 1249.6 $cm^{-1}$ (amide III). Also, the stretching peak at 3384.2 $cm^{-1}$ can be assigned to N–H (and O–H) and suggests several loose associative features like NH–N hydrogen bonds as also NH–O=C hydrogen bonds. Fig. 2 also shows that the FT-IR spectra for membranes loading with

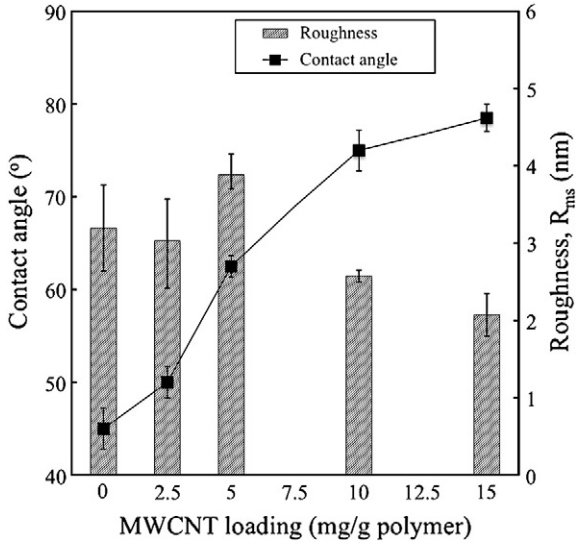


**Fig. 3.** Effects of MWCNTs loadings on surface properties of the nanocomposite membrane.

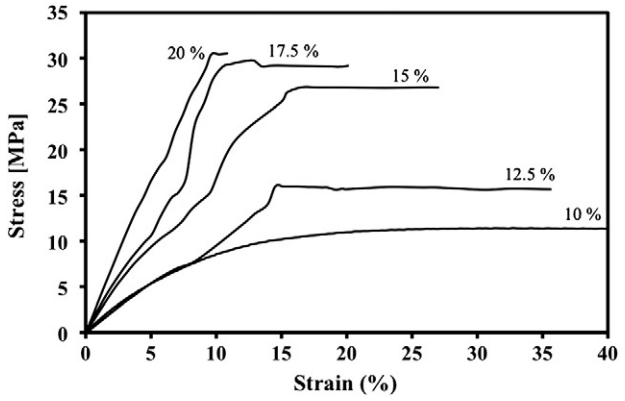


**Fig. 4.** Stress–strain curves for control membranes of different PA concentrations.

various concentrations of MWCNTs are almost identical with that of the blank membrane.

*3.2.2. Surface properties*

The contact angle increased from approximately 45° to 75° as the fraction of MWCNTs in the membrane increased from 0 to 10 mg/g (Fig. 3). These results are consistent with the hydrophobic nature of fullerene nanomaterials [21–23]. However, it is notable that such a significant difference in contact angle is produced at small concentrations of MWCNTs. As shown in Fig. 3, the surface roughness of the composite membranes with and without CNTs were similar or perhaps slightly less in the MWCNT composite membranes, supporting the visual observation that the MWCNTs were well dispersed in the polymer matrix.

*3.2.3. Mechanical properties*

Mechanical testing on rectangular strips of the pure polyamide was carried out at 25 °C. Fig. 4 shows the general shape of the stress–strain curves of the synthesized PA membranes with various concentrations of PA ranging from 10 to 20% in the casting solution. These curves exhibit an initial linear portion typical of the elastic response, then curvature corresponding to the inelastic response before the yield point is attained at the maximum stress, and finally some strain softening. Table 1 summarizes the mechanical properties of the PA membrane without CNTs. The Young's modulus is calculated from the initial slopes of the linear portion of the stress–strain isotherm. Also, toughness of the membranes is determined by integrating the area under the stress–strain isotherm up to maximum extension, which correspond to the energy or work required for rupture [24,25]. From Table 1 it can be seen that increasing the polymer concentration from 10 to 20% results in an increase in both maximum strength (11.3 to 30.5 MPa) and Young's modulus (97.8 to 348.3 MPa). On the other hand, this increase in polymer concentration leads to a decrease in elongation from 40 to 9.6% and a drop in the toughness from 4.4 to 1.9 MPa. These latter results are consistent with an increasingly rigid aromatic structure higher intermolecular stiffness with increasing PA concentration [26]. An increase in rigidity is typically accompanied by a decrease in the membrane elasticity leading to a decrease in the elongation and toughness [24–26].

**Table 1**
Mechanical characteristics of the synthesized membranes.

| Sample | | Tensile strength [MPa] | Elongation [%] | Young's modulus [MPa] | Toughness [MPa] |
|---|---|---|---|---|---|
| Polyamide concentration (%) | 10 | 11.3 | 39.8 | 97.8 | 4.4 |
| | 12.5 | 15.6 | 35.6 | 128.1 | 4.3 |
| | 15 | 26.7 | 26.9 | 201.4 | 4.1 |
| | 17.5 | 29.2 | 20.1 | 214.1 | 3.8 |
| | 20 | 30.5 | 10.8 | 348.3 | 1.9 |
| MWCNTs loading (mg/g) | 2.5 | 13.4 | 39.8 | 210.2 | 4.7 |
| | 5 | 13.3 | 39.8 | 210.4 | 4.6 |
| | 10 | 24.1 | 39.5 | 316.8 | 7.9 |
| | 15 | 34.3 | 39.4 | 491.2 | 11.3 |

**Table 2**
Control membrane RO performance as a function of different PA concentrations.

| PA concentration (%) | Permeability ($L/m^2$ h bar) | Flux ($L/m^2$ h) | Salt rejection (%) |
|---|---|---|---|
| 10 | 0.76 ± 0.08 | 32 ± 0.7 | 24 ± 1.1 |
| 12.5 | 0.54 ± 0.10 | 22 ± 0.9 | 27 ± 0.9 |
| 15 | 0.45 ± 0.09 | 19 ± 0.4 | 31 ± 1.0 |
| 17.5 | 0.35 ± 0.11 | 14 ± 0.8 | 55 ± 0.8 |
| 20 | 0.28 ± 0.04 | 11 ± 0.5 | 65 ± 0.7 |

Stress–strain measurements were also performed on the synthesized MWCNTs-PA composite membranes where the PA was present at a concentration of 10%. The addition of CNTs to the membrane considerably improved the mechanical properties of the membrane (Fig. 5). Compared with the 10% PA-derived membrane the MWCNT/PA composite exhibited a monotonically increasing Young's modulus and toughness with MWCNT content (Table 1). The increase in MWCNTs loading from 0 to 15 mg MWCNT/g PA in the membrane increased membrane strength from 11.3 to 34.3 MPa and the Young's modulus from 97.8 to 491.2 MPa. In addition, a significant increase in toughness, from 4.4 to 11.3 MPa was observed. Furthermore, no significant decrease in elongation was observed, dropping from 39.8 to 39.4% over the range of MWCNT treatments.

Coleman et al. [2] used the rate of increase of Young's modulus with volume fraction $dY/dV_F$ as a yardstick for reinforcement. Thus, the increase in moduli with the increase in PA concentration from 10 to 20% in the membranes without CNTs is equivalent to a reinforcement value of $dY/dV_F = 25$ GPa. Meanwhile, a reinforcement value of $dY/dV_F = 262.2$ GPa corresponds to the increase in MWCNTs loading from 0 to 15 mg/g in the nanocomposite membrane. These impressive improvements in mechanical properties of the membrane may be attributed to the strong interactions between the polyamide matrix and MWCNTs and homogeneous dispersion and adhesion of CNTs, as observed by microscopy measurements (Figs. 1 and 3).

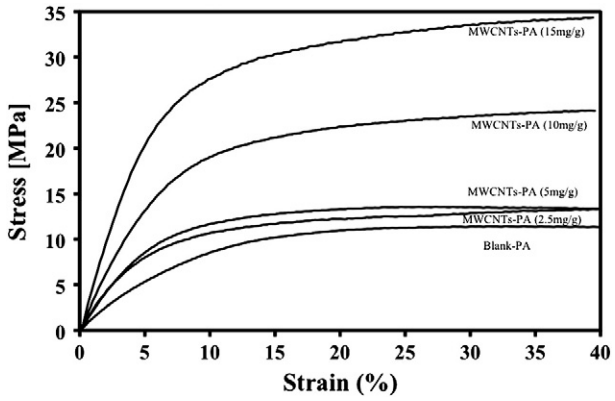


**Fig. 5.** Effect of MWCNTs contents on the stress–strain curves for PA membranes.

**Table 3**
Membrane performance as a function of different MWCNTs loading at constant PA concentration (10%).

| MWCNTs loading (mg/g) | Permeability ($L/m^2$/h bar) | Flux ($L/m^2$ h) | Salt rejection (%) |
|---|---|---|---|
| 0 | 0.76 ± 0.08 | 32 ± 0.7 | 24 ± 1.1 |
| 2.5 | 0.75 ± 0.09 | 32 ± 0.4 | 28 ± 1.0 |
| 5 | 0.73 ± 0.07 | 31 ± 1.1 | 35 ± 0.7 |
| 10 | 0.72 ± 0.10 | 30 ± 0.9 | 69 ± 0.9 |
| 15 | 0.71 ± 0.11 | 28 ± 0.8 | 76 ± 1.1 |

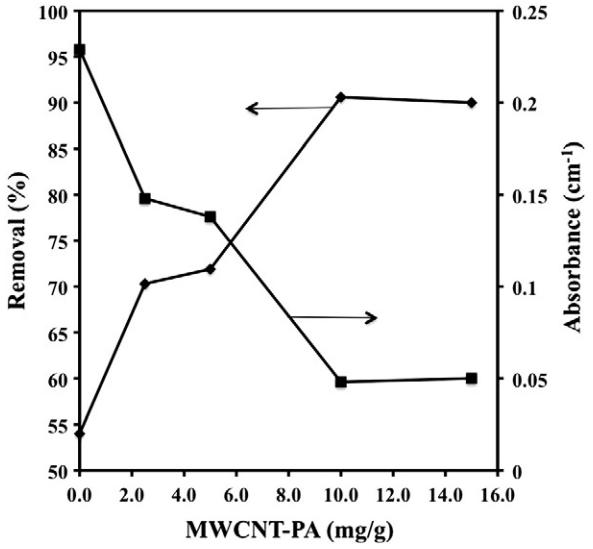


**Fig. 6.** Removal efficiency of humic acid (initial concentration = 20 ppm, UV254 = 0.499) by different MWCNT-PA nanocomposite membranes at 40 bar.

### 3.3. Effect of MWCNT content on membrane permeability and rejection

Salt rejection, and pressure-normalized water flux (specific flux) were measured for both the PA and MWCNT/PA composite membranes. An increasing PA concentration in membrane casting solution, produced an increase in salt rejection from 24 to 64.5% accompanied by a decrease in both permeability and specific flux which drop from 0.76 to 0.28 L/m$^2$ h bar and from 32 to 11 L/m$^2$ h, respectively (Table 2). These salt rejections are relatively low compared with commercially available PA membranes that typically show rejections in excess of 90% for NaCl. The incorporation of MWCNTs into the 10% PA membranes increased salt rejection significantly with a small sacrifice in permeate flux (Table 3). The addition of MWCNTs to the 10% PA membrane increased salt rejection to 76% while specific flux dropped from 0.76 to 0.71 L/m$^2$ h bar in the case of the 15 mg/g MWCNTs-PA. Indeed, the salt rejection by this membrane exceeded that of the 20% PA membrane without CNTs. The addition of MWCNT causes a structural compactness of the composite membranes as a result of the strong interaction between MWCNTs and PA matrix suggesting a network structure [1,4]. This network structure increases with increasing the amount of CNTs in the composite. Thus, the lower permeability and higher salt rejection may be attributed to this network structure [26,27]. Given that the significant removal of NaCl was observed using all of the membrane tested, it is not surprising that these membranes also removed the relatively large-molecular weight humic acid. Humic acid removal by the MWCNT composite membranes increased from 54 to 90% as the MWCNT loading increased from 0 to 10 mg/g (Fig. 6).

## 4. Conclusion

The addition of MWCNTs to the PA membranes to form a nanocomposite structure improved the mechanical properties of these membranes and their ability to reject key contaminants with little compromise in membrane permeability. However, there may be a reduction in longer-term membrane performance due to adsorptive fouling since the addition of MWCNTs increased membrane hydrophobicity. Additional factors to consider in the development of these composites include the need to balance the dimensions of the membrane film cast with those of the reinforcing CNTs, and the effect of derivative CNTs on membrane casting and performance.

## References

[1] R. Song, D. Yang, L. He, Preparation of semi-aromatic polyamide(PA)/multi-wall carbon nanotube (MWCNT) composites and its dynamic mechanical properties, J. Mater. Sci. 43 (2008) 1205–1213.
[2] J.N. Coleman, U. Khan, Y.K. Gun'ko, Mechanical reinforcement of polymers using carbon nanotubes, Adv. Mater. 18 (2006) 689–706.
[3] Z. Yang, Z. Cao, H. Sun, Y. Li, Composite films based on aligned carbon nanotube arrays and a poly(N-isopropyl acrylamide) hydrogel, Adv. Mater. 20 (2008) 2201–2205.
[4] W. Li, X. Chen, C. Chen, L. Xu, Z. Yang, Y. Wang, Preparation and shear properties of carbon nanotubes/poly(butyl methacrylate) hybrid material, Polym. Compos. 29 (9) (2008) 972–977.
[5] L. Brunet, D.Y. Lyon, K. Zodrow, J.-C. Rouch, B. Caussat, P. Serp, J.-C. Remigy, M.R. Wiesner, P.J.J. Alvarez, Properties of membranes containing semi-dispersed carbon nanotubes, Environ. Eng. Sci. 25 (4) (2008) 1–11.
[6] M.J. O'Connell, P. Boul, L.M. Ericson, C. Huffman, Y.H. Wang, E. Haroz, C. Kuper, J. Tour, K.D. Ausman, R.E. Smalley, Reversible water-solubilization of single-walled carbon nanotubes by polymer wrapping, Chem. Phys. Lett. 342 (2001) 265–271.
[7] M.F. Islam, E. Rojas, D.M. Bergey, A.T. Johnson, A.G. Yodh, High weight fraction surfactant solubilization of single-wall carbon nanotubes in water, Nano Lett. 3 (2003) 269–273.
[8] Z. Yang, X.H. Chen, C.S. Chen, W.H. Li, H. Zhang, L.S. Xu, B. Yi, Noncovalent-wrapped sidewall functionalization of multiwalled carbon nanotubes with polyimide, Polym. Compos. 28 (2007) 36–41.
[9] S. Kwak, Relationship of relaxation property to reverse osmosis permeability in aromatic polyamide thin-film-composite membranes, Polymer 40 (1999) 6361–6368.
[10] N.A. Mohamed, A. Al-Dossary, Structure-property relationships for novel wholly aromatic polyamide-hydrazides containing various proportions of *para*-phenylene and *meta*-phenylene units III. Preparation and properties of semi-permeable membranes for water desalination by reverse osmosis separation performance, Eur. Polym. J. 39 (2003) 1653–1667.
[11] B.E. Kilbride, J.N. Coleman, J. Fraysse, P. Fournet, M. Cadek, A. Drury, S. Hutzler, S. Roth, W.J. Blau, Experimental observation of scaling laws for alternating current and direct current conductivity in polymer-carbon nanotube composite thin films, J. Appl. Phys. 92 (2002) 4024–4030.
[12] M. Cadek, J.N. Coleman, V. Barron, K. Hedicke, W.J. Blau, Morphological and mechanical properties of carbon-nanotube-reinforced semicrystalline and amorphous polymer composites, Appl. Phys. Lett. 81 (2002) 5123–5125.
[13] M. Cadek, J.N. Coleman, K.P. Ryan, V. Nicolosi, G. Bister, A. Fonseca, J.B. Nagy, K. Szostak, F. Beguin, W.J. Blau, Glucose biosensors based on carbon nanotube nanoelectrode ensembles, Nano Lett. 4 (2004) 353–356.
[14] J.N. Coleman, M. Cadek, R. Blake, V. Nicolosi, K.P. Ryan, C. Belton, A. Fonseca, J.B. Nagy, Y.K. Gun'ko, W.J. Blau, High performance nanotube-reinforced plastics: understanding the mechanism of strength increase, Adv. Funct. Mater. 14 (2004) 791–798.
[15] F. Dalmas, L. Chazeau, C. Gauthier, K. Masenelli-Varlot, R. Dendievel, J.Y. Cavaillé, L. Forró, Multiwalled carbon nanotube/polymer nanocomposites: processing and properties, J. Polym. Sci. B Polym. Phys. 43 (2005) 1186–1197.
[16] A. Dufresne, M. Paillet, J.L. Putaux, R. Canet, F. Carmona, P. Delhaes, S. Cui, Processing and characterization of carbon nanotube/poly(styrene-co-butyl acrylate) nanocomposites, J. Mater. Sci. 37 (2002) 3915–3923.
[17] B. McCarthy, J.N. Coleman, R. Czerw, A.B. Dalton, M.I.H. Panhuis, A. Maiti, A. Drury, P. Bernier, J.B. Nagy, B. Lahr, H.J. Byrne, D.L. Carroll, W.J. Blau, A microscopic and spectroscopic study of interactions between carbon nanotubes and a conjugated polymer, J. Phys. Chem. B 106 (2002) 2210–2216.
[18] X. Xu, R.J. Kirkpatrick, NaCl interaction with interfacially polymerized polyamide films of reverse osmosis membranes: a solid-state $^{23}$Na NMR study, J. Membr. Sci. 280 (2006) 226–233.
[19] S. Kim, L. Chen, J.K. Johnson, E. Marand, Polysulfone and functionalized carbon nanotube mixed matrix membranes for gas separation: theory and experiment, J. Membr. Sci. 294 (2007) 147–158.
[20] A.H. Liu, I. Honma, M. Ichihara, H.S. Zhou, Poly(acrylic acid)-wrapped multi-walled carbon nanotubes composite solubilization in water: definitive spectroscopic properties, Nanotechnology 17 (2006) 2845–2849.
[21] C.H. Xue, M.M. Shi, Q.X. Yan, Z. Shao, Y. Gao, G. Wu, X.B. Zhang, Y. Yang, H.Z. Chen, M. Wang, Preparation of water-soluble multi-walled carbon nanotubes by polymer dispersant assisted exfoliation, Nanotechnology 19 (2008) 1–7.
[22] S. Deguchi, R.G. Alargova, K. Tsujii, Stable dispersions of fullerenes, C-60 and C-70, in water. Preparation and characterization, Langmuir 17 (2001) 6013–6017.
[23] S. Zulfiqar, M.I. Sarwar, Soluble aromatic polyamide bearing sulfone linkages: synthesis and characterization, High Perform. Polym. 21 (2008) 3–15.
[24] S. Zulfiqar, Z. Ahmed, M.I. Sarwar, Soluble aromatic polyamide bearing ether linkages: synthesis and characterization, Colloid Polym. Sci. 285 (2007) 1749–1754.
[25] H. Wang, M. Lin, Modification of Nylon-6 with semi- or wholly-aromatic polyamide, J. Polym. Res. 5 (1) (1998) 51–58.
[26] S.Y. Lee, H.J. Kim, R. Patel, S.J. Im, J.H. Kim, B.R. Min, Silver nanoparticles immobilized on thin film composite polyamide membrane: characterization, nanofiltration, antifouling properties, Polym. Adv. Technol. 18 (2007) 562–568.
[27] C.K. Kim, J.H. Kim, I.J. Roh, J.J. Kim, The changes of membrane performance with polyamide molecular structure in the reverse osmosis process, J. Membr. Sci. 165 (2000) 189–199.